SS Project Report

Metal and Semiconductor based Nanomaterials: Synthesis and Assembly

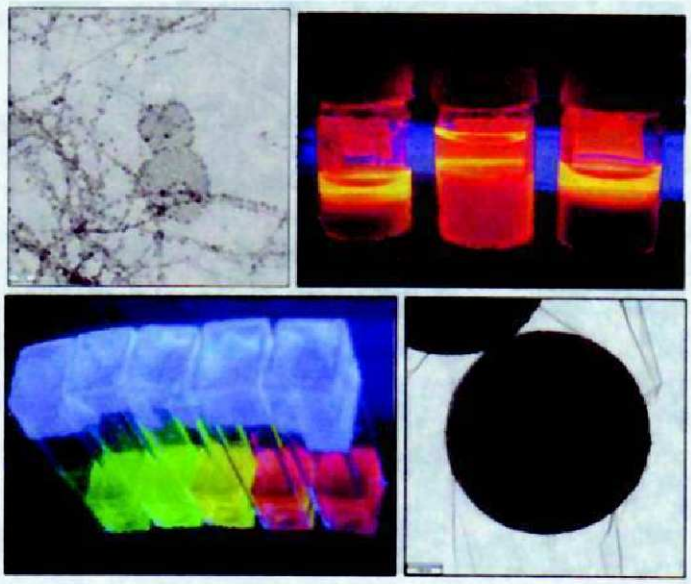

PhOG,

December 2006

Acknowledgements

I would like to thank Prof. for providing me with an opportunity to join his group for my SS project. I sincerely thank my supervisor Dr. for his invitation and the organization of my stay in and also for scientific guidance.

Special thanks to Dr. for his supervision and help with the experimental part of the project, and also for showing me Munich and surrounding areas. I thank for the always appreciated experimental tips and other discussions. is acknowledged for his help with photovoltaic measurements.

I thank everybody in the group for making this experience an enjoyable one. Above all I would like to thank my family for their love and support.

Index:

Abbreviations and Notations

#	Footnote
λ_{max}	Wavelength at which the maximum of a PL peak occurs
ABS	Absorbance
CdSe	Cadmium Selenium
CdTe	Cadmium Telluride
DMAP	4-dimethylaminopyridine
FOG	Free Organic Group
FRET	Foster Resonant Energy Transfer
LA	α-Lipoic Acid
LBL	Layer-by-layer
MES	Sodium 2-Mercaptoethanesulfonate
MF spheres	Melamine formaldehyde particles (positively charged, weakly cross-linked)
MPA	3-Mercaptopropionic Acid
NC	Nanocrystal
NP	Nanoparticle
PAH	Poly(allylamine hydrochloride)
PE	Polyelectrolyte
PL	Photoluminescence
PS spheres	Polystyrene latex particles (negatively charged, sulphate-stabilized)
PSS	Poly(styrenesulfonate)
QD	Quantum Dot
QY or QE	Quantum Yield (or Efficiency)
TEM	Transmission Electron Microscopy
TGA	Thioglycoic Acid
TOAB	Tetraoctylammonium bromide
UV-vis	Ultraviolet-visible

1. Abstract

This project involved an investigation into the synthesis and layer-by-layer assembly of metal and semiconductor nanoparticles. Aqueous colloidal gold was fabricated by previously reported method, and later assembled on latex microspheres of different diameters. The microwave-assisted synthesis of glycine-stabilised CdSe nanocrystals was successfully accomplished under various reaction conditions, to produce superstructures whose morphology can be controlled. Lipoic acid and sodium 2-mercaptoethanesulphonate (MES) were tested as novel stabilizers for CdTe nanocrystals. Lipoic acid was found to be inadequate for such use, but syntheses of MES-stabilized CdTe were successful. Highly luminescent CdTe nanocrystals, both as colloidal solutions and also in precipitates, with quantum efficiencies of up to 40% were produced. Finally, layer-by-layer technique was used to assemble monolayers of TGA-stabilized CdTe on latex microspheres.

2. Introduction

Nowadays, nanoparticle research is an interdisciplinary subject. Solid-state physicists, inorganic, physical and colloidal chemists, material scientists, biologists, medics and engineers often work in tandem to further progress this highly dynamic research field. This immense and varied interest in nanoscience arises from the finding that many properties of nanoscale materials are determined not only by their chemical composition but also by their size. Such properties include the melting point and phase transition temperature of a material, and also their optical, catalytic, magnetic and electronic behavior [1]. Hence, nanoparticles, with sizes in the 1-100nm range, represent an intermediate state of matter between a bulk solid and a molecule.

By far the oldest topic in this field has been the study of metal nanoparticles (gold and silver), whose size-dependent optical properties were reported more than 150 years ago [2]. Such properties arise because the diameter of metal nanoparticles is much smaller than the wavelength of light, and so they are easily penetrated by electromagnetic waves. This creates an electric field within a particle that deflects conduction electrons. A restoring force arises due to the displacement of charges, and this sets up a coherent oscillation of conduction electrons around their equilibrium position. These collective oscillations of electron density on the surface of a metal particle are termed surface or particle plasmons [3]. For gold and silver nanoparticles, plasmon resonance is usually in the visible region. Resonant excitation of particles strongly raises their extinction coefficient, and hence plasmon resonance is readily observed by absorption spectroscopy.

The second, relatively more recent topic in the field of nanoscience is that of semiconductor nanocrystals (1-10nm), otherwise known as quantum dots. These owe their size-dependent electronic and optical properties to the fact that their lattice size is smaller than the exciton Bohr radius[#]. This confines the excited charge carriers independently, resulting in the appearance of discrete electronic energy levels (molecular orbitals) [4]. Similar to the case of a particle-in-a-box problem, the spacing of these levels increases with decreasing particle size. By adjusting the physical size of the nanocrystal, its band-gap energy, and hence the frequency of a photon emitted upon the annihilation of an electron-hole pair, can be tuned over a very broad frequency range.

[#] Exciton Bohr radius is the radius of a bound electron-hole pair in a semiconductor.

Due to their unique properties, the applications of both metal and semiconductor nanoparticles have been, and continue to be extensively studied. Currently, gold NPs are used in decorative metal paints, catalysts, gas sensors and as biosensors; while investigations are under way into their potential use in ink-jet printing of conductive structures, small electronic devices (e.g. one electron transistors), polarizing filters and nanodiagnostics. Semiconductor nanocrystals, on the other hand, were already successfully used as bio-labeling and cell-imaging agents. Potential applications of QDs are diverse and include their use in LEDs, solar cells and telecommunication amplifiers.

The production of stable, high quality[#] NCs/NPs is the first and very important step towards the realization of their potential uses. The aim of this project was thus to investigate the syntheses of Au NPs, CdSe and CdTe NCs, and, in some cases, their assembly to produce potentially useful superstructures. In particular, aqueous colloidal gold nanoparticles were produced and characterized using both transmission spectroscopy and transmission electron microscopy (TEM). Microwave-assisted method was then investigated as means of glycine-stabilised CdSe production. Finally, two new stabilizers for CdTe NCs were tested.

[#] Here, for both metal and semiconductor nanoparticles, high quality means desired particle size over the largest possible range, narrow size distributions, controllable surface functionalisation. For semiconductor nanoparticles, high crystallinity and quantum yields are also implied. [5]

3. Topic review

As already mentioned before, this project concentrated mainly on the synthesis of nanoparticles and their assembly. Most known procedures for NC/NP production can be divided into the physical (top-down) and chemical (bottom-up) methods. Top-down techniques are usually lithography-related and are often restricted by the limits of equipment used (e.g. diffraction limit). The chemical approach, on the other hand, is often a colloidal method, in which nanoparticles are produced in liquid media and are kept in suspension by the so-called stabilizers. All NPs/NCs produced as part of this project were synthesized by a colloidal method. For this reason, this short review focuses mainly on the existing methods of colloidal gold and semiconductor nanocrystals preparation.

3.1 Colloidal Nanoparticles and the Role of Stabilizers.

Nanoparticles prepared by a colloidal method present a system in which each nanoparticle is capped by molecules that, through either non-polar or polar interactions, prevent the aggregation of the nanoparticles and thus keep them suspended in solution. Many properties of nanoparticles depend on these stabilising molecules. Such properties include solubility, stability, charge and biocompatibility. The broader the range of available stabilizers, the broader is the range of NP's properties.

3.2 Synthesis of Gold Nanoparticles

Colloidal gold was used as early as 4th century AD for decorative properties [6]. However, it was not until 1857 that Michael Faraday recognised that the gold in a colloidal solution was present in a metallic state. Even then, a few different methods of colloidal gold production existed; Faraday himself has developed several new physical and wet-chemical methods [7]. Today, the synthesis of gold nanoparticles can be achieved by a variety of different techniques.

The most common method used today is Turkevich's modification [8] of Hauser and Lynn's citrate reduction route, first reported in 1940 [9]. In this method, particles grow through the reduction of gold salt by citrate. By changing the ratio of gold to citrate, the order of addition of the reagents and/or the temperature of reacting solution, very uniform gold nanoparticles of 10-40nm in diameter can be produced.

Another popular technique for the generation of large, nearly monodisperse colloidal gold is the "seeded-growth" method, first introduced by Zsigmondy [10] in 1906. Here, a very strong

reducing agent, such as sodium borohydride, is first used to produce very small seed colloids. These "seeds" are then transferred to a growth solution, which employs a weaker reducing agent that is only capable of reducing the metal (present as salt) to an intermediate state [11]. Under these conditions, the nucleation of new particles is prohibited and thus the reduction of metal is only possible on the surface of seed colloids, i.e. via their growth.

The next breakthrough in colloidal gold preparation came with the discovery that organic sulphur compounds spontaneously assemble on gold surfaces [12] (Nuzzo, Allara, 1983). This fuelled the development of thiol-stabilization as means of production of highly stable, small (1-5nm) and monodisperse gold colloids. In fact, the stability of such NPs is by far superior to that of colloidal gold produced by any other method. Giersig and Mulvaney were the first to successfully stabilize gold nanoparticles by thiols [13] in 1993, and in 1994 a relatively simple two-phase method of thiol-stabilized colloidal gold production was developed by Schiffin et al. [14]. The reagents were introduced to the aqueous phase and later transferred to an organic phase (toluene) by aid of tetraoctylammonium bromide, where the reduction of the gold complex took place. To date, many different improvements and modifications of this method were reported [15].

Another area, that has received a lot of attention over the years, has been that of phase transfer of produced nanoparticles to other solvent media, i.e. from aqueous to organic and vice-versa. Many procedures exist today, with the majority concentrating on the transfer of particles from aqueous to organic media [16]. On average, however, organic syntheses allow better control over size and shape of nanoparticles and often lead to better monodispersity and higher concentrations of colloid solutions. The first reported methods for phase transfer from organic to aqueous media often involved irreversible covalent capping of nanoparticles [17] through a series of precipitation steps and solvent exchanges [18]. In 2001, Gittings and Caruso reported the first facile one-step method of particle transfer from organic (toluene) to aqueous media [19], which was employed in this project.

3.3 Synthesis of Semiconductor Nanocrystals

Among all the different areas of colloidal science, the topic of semiconductor nanocrystals is probably one of the most recent. The first ever method of colloidal quantum dot preparation was reported in 1982 by Henglein [20]. In this method, CdS nanocrystals were formed by mixing of cadmium and sulfide salts in an aqueous buffer. Since then, two general synthetic

procedures for quantum dot production have emerged – the organometallic synthesis and the aqueous synthesis.

The organometallic synthesis, developed by Murray et al. [21], involves a high-temperature (200-360°C) thermolysis of precursors in organic coordinating solvents (stabilizers) [5]. Organometallic precursors are added to a very hot solution of stabilizers (e.g. TOPO-TOP at ~300-320°C for CdSe) which causes an explosive nucleation of semiconductor nanocrystallites. Next, temperature drop to ~200°C terminates the nucleation and is followed by a slow growth of the nuclei. Due to the high temperatures involved, this method results in nanocrystals having a very high crystallinity. To achieve high quantum yields, however, it is often important to passivate surface defects of nanocrystals through capping with a material of larger band-gap. For example, CdSe nanocrystals are commonly capped by CdS or ZnS [5].

The aqueous synthesis often involves the use of thiols as stabilizers. Syntheses of different nanocrystals involve slightly different procedures and precursors [5]. Generally, for CdS, CdSe and CdTe, Cd salt and stabilizer are dissolved in water and S, Se or Te precursor is bubbled through the solution (respectively) causing the nucleation of crystals to occur. The growth of the nanocrystals is achieved through the application of heat. In this project, an aqueous synthesis first reported in 1996 [22] was used to produce CdTe nanocrystals and a microwave-assisted synthesis [23] was employed for CdSe quantum dot fabrication.

3.4 Layer-by-Layer Assembly

Layer-by-layer (LBL) assembly is a very successful technique for the adsorption of sequential ultra-thin layers of material on substrates. It was developed in the early 1990s [24], and it uses the electrostatic attraction between oppositely charged species as the driving force for monolayer build-up [25]. In short, the electrostatic attraction between ions (or other charged species, s.a. colloids) in solution and an oppositely charged substrate surface causes the adsorption of charged species from solution onto a substrate. This, of cause, results in the reversal of substrate's surface charge, so that adsorption of another layer of oppositely charged species is now possible. The LBL technique was used successfully in the project to assemble both gold NPs and CdTe NCs onto latex microspheres.

4. Research techniques

4.1 General Procedures

All chemicals used were chemical grade and were purchased from Sigma-Aldrich or VWR. Al_2Te_3 was purchased from CERAC Inc. and used as received. For all dilutions, washes and solution preparations, millipore water from a MilliQ system was used.

The transmission electron microscopy images were obtained on a JEM 1011 (JEOL Ltd., Japan) at either 80 or 100kV. Samples for the TEM were prepared by placing a 5 μL drop of sample to be examined onto carbon-coated TEM grid and removing excess water after 2-3 minutes by touching a filter paper.

UV-vis absorption spectra were collected with a Carry 500 (Varian) spectrophotometer. Samples' dilution was such that the absorbance at peak did not exceed 0.2 in order to eliminate the re-absorption effects. Photoluminescence measurements were done on a Fluoromax-2 (Instruments SA) spectrofluorimeter. Centrifugation of samples of small volumes was performed on a MiniSpin200. Samples of larger volumes were centrifuged on a Beckman-Coulter Optima XL-I ultracentrifuge.

The quantum yield of CdTe nanocrystals was measured against a Rhodamine 6G in absolute alcohol standard which has a 95% QE for 248-528nm excitation wavelengths [26]. Both the Rhodamine 6G solution and the colloidal CdTe NCs were diluted so that their absorbance spectra intersected at 470-480nm region with the absorbance below 0.15 at that point. Photoluminescence spectra of both solutions were then taken, exciting the samples at the intersection wavelength. The QY of CdTe NCs was then calculated by multiplying the ratio of NCs to Rhodamine 6G integrated areas by the QY of the dye (i.e. 95%).

Photoelectrical measurements were performed as reported before for the photoelectrical measurements of C_{60}/QDs mixtures [27]. To prepare samples for these measurements, 10μL of previously shaken test solution were drop-casted onto interdigitating finger-like gold contacts on glass slides with 5-10 μm spacing between the fingers (a representative sample is shown on the right).

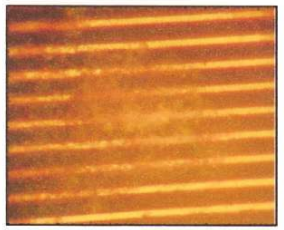

Fig. 4.1 A microscopic image of a representative sample for the electrical measurements: CdSe precipitate on top of interdigitating finger-like gold contacts.

Zeta potential and size measurements were performed on a Malvern ZEN3600 ZetaSizer. Only appropriate dilution of samples was necessary for these measurements.

4.2 Gold Nanoparticles

Colloidal gold nanoparticles were prepared by two-step synthesis, i.e. they were first synthesised in toluene and then transferred to aqueous media by a 4-dimethylaminopyridine (DMAP)–induced spontaneous phase transfer [19]. The fabricated gold nanoparticles were subsequently used to coat latex microspheres of various diameters by a layer-by-layer (LBL) assembly technique [25,28,29].

4.2.1 Synthesis

30mL of aqueous 30mM $HAuCl_4$ was added to 80mL of a 25mM TOAB solution in toluene. The transfer of metal salt to toluene salt was easily observed through colour change with the aqueous phase going clear and the organic phase acquiring a deep red colour: $HAuCl_4 + BrNR_3 \rightarrow H^+ + Cl^- + Br^- + Au{:}NR_3$. The mixture was washed with water until the pH of the aqueous phase reached 5-6. The aqueous phase was then separated out, leaving the organic mixture containing Au ions. To this stirred mixture, 30ml of aqueous 0.25M $NaBH_4$ solution was added dropwise. This caused a reduction reaction to occur with a colour change from deep red to deep blue/violet. The reacted mixture was then washed with water several times, until the pH of the aqueous phase was about 6. A phase transfer of gold nanoparticles was then carried out by addition of 80ml of aqueous 0.1M DMAP solution.

4.2.2 LBL Assembly of Gold NPs on Latex Microspheres.

First, a precursor polyelectrolyte (PE) layer (PAH-PSS-PAH-PSS-PAH) was formed by alternative adsorption of PAH and PSS onto MF lattices from 1mg/mL aqueous solutions of corresponding polyelectrolytes in 0.5M NaCl. The adsorption time for each electrolyte layer was 15min. Excess PE was removed each time by four centrifugation/re-dispersion cycles (speed and time of the centrifugation depended on the size of the latex microspheres; samples were re-dispersed once with 0.15M NaCl and three times with water). Gold layer was next formed on the MF lattices by adding colloidal gold solution (obtained as described in the previous section) and leaving the mixture overnight to allow the adsorption of gold nanoparticles. The concentration of gold used was much higher than that required to form a monolayer. Excess of gold was then removed by four centrifugation (1000rpm, 3mins)/redispersion with water cycles. The procedure was repeated until the desired structure was achieved, adsorbing 4 PE layers between gold multilayers.

4.3 Synthesis of Glycine-Stabilized CdSe

The microwave-assisted synthesis of glycine-stabilized CdSe performed was analogous to that reported before for the synthesis of citrate-stabilized CdSe nanocrystals [23].

4.3.1 Synthesis

4-16mL of 40mM $Cd(ClO_4)_2$ aqueous solution was added to 90mL of 36mM aqueous glycine solution – this corresponds to about 1-4 moles of Cd to every 20 moles of stabilizer. The pH of the solution was adjusted to the desired value (typically 9.0, but also 7.0 or 10.0) using 0.1M NaOH. The resulting solution was bubbled with nitrogen for 10 minutes. 4mL of 10mM N,N-dimethylselenourea was added and the mixture was heated in a 900W conventional microwave oven for up to 10 minutes (depending on how fast the evaporation of the mixture took place). 3mL of reacting solution were taken out at 1 minute intervals for spectral analysis.

4.4 CdTe Synthesis and Assembly

The fabrication of CdTe QDs was attempted by a previously published aqueous method [22] using various substances as stabilizers. These or other nanocrystals were subsequently used to produce thin films of CdTe nanocrystals on spherical (latex microspheres) substrates by the LBL assembly approach.

4.4.1 Synthesis

0.985g of $Cd(ClO_4)_2.6H_2O$ was dissolved in 125mL of water, stabilizer was added under stirring. The pH of the solution was adjusted to the desired value by a dropwise addition of 0.1M NaOH. The reaction mixture was then transferred into a double-necked round-bottom flask and the apparatus was set up as shown in diagram 4.1a, with approximately 0.2g of Al_2Te_3 added to the small round-bottom flask. The system was deaerated by bubbling nitrogen gas through for 30 minutes. 7-8ml of deaerated H_2SO_4 were subsequently added dropwise to the flask containing Al_2Te_3. The reaction between the two generates H_2Te gas which is passed through the reaction solution together with a slow nitrogen flow for about 20 minutes. As H_2Te gas passes through the solution, a colour change is observed, which is due to the formation of CdTe clusters. These precursors are then converted to CdTe nanocrystals by refluxing the reaction mixture at 100°C under open-air conditions (diagram 4.1b). The size of the produced CdTe QDs is controlled by the duration of the reflux.

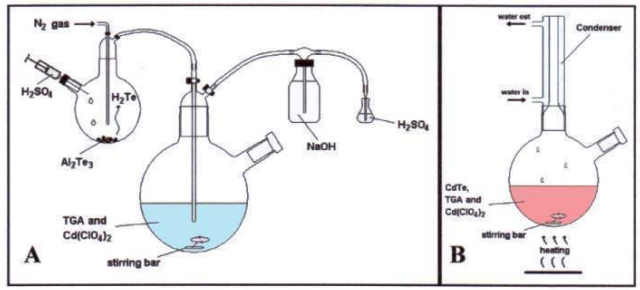

Diagram 4.1. Apparatus set up for (a) the initial stages of the synthesis and (b) the refluxing of the reacting mixture during which CdTe NCs grow.

4.4.2 Post-Preparative Size-Selective Precipitation of CdTe NCs

Crude, as-prepared, CdTe solution was first concentrated using a rotary evaporator (35°C, 30mins). 2-propanol was then added dropwise under stirring until the solution became slightly turbid. After 15 minutes of stirring, the first fraction of CdTe nanocrystals was isolated from the supernatant by centrifugation (4 minutes at 4500 rpm). The isolated CdTe nanocrystals were re-dispersed in water, while 2-propanol was added dropwise to the supernatant until slightly turbid. After 15 minutes the second fraction was isolated from the supernatant. This procedure was repeated until up to 8 fractions of CdTe nanocrystals were obtained.

4.4.3 LBL Assembly of CdTe Nanocrystals

The procedure for the deposition of PE/CdTe NC layers on PS latex microspheres was identical to LBL assembly of PE/Au NPs multilayers on MF microspheres, albeit the adsorption time for each NC layer was 40 minutes and that for each PE layer was 20 minutes.

5. Experimental Results and their Discussion

5.1 Colloidal Gold

Aqueous colloidal gold was fabricated by a two-step synthesis [19]. The two-step synthesis was used as it yields relatively high concentration of gold NPs in aqueous media when compared to other water-based syntheses of gold nanoparticles.

An absorption spectrum of a synthesized sample is shown in Fig. 5.1. A plasmon resonance peak can be clearly resolved at 520 nm.

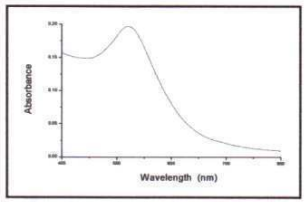

Figure 5.1. Absorbance spectrum of a representative colloidal gold sample.

Synthesized gold NPs were examined using the transmission electron microscopy. From the TEM images (fig. 5.2a), the average diameter of nanoparticles was found to be ~4.7 nm. However the standard deviation for this was 1.3 nm, which is indicative of a rather large spread of particle sizes. To give an estimate of this spread, the diameter data obtained from TEM images was used to compose a histogram of nanoparticle sizes (shown in fig. 5.2b). As seen from the histogram, the size of synthesized NPs ranged from 1nm to about 8nm.

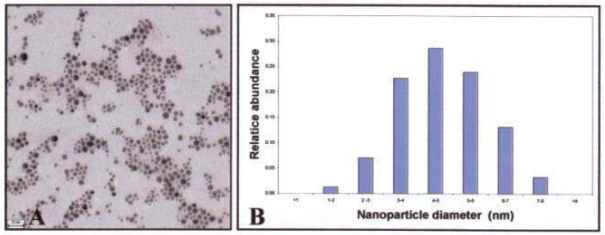

Fig. 5.2. (a) A TEM image and (b) a size histogram of synthesised gold nanoparticles.

The prepared NPs can be functionalized for various applications including biodiagnostics, catalysis and optical application [11]. One such application involves the enhancement/quenching of molecular chromophores (dyes) when located in vicinity of a nanostructured Au film or free gold NPs (in solution). Similar photoluminescence quenching/enhancement effect can also be observed for CdTe nanocrystals placed in the proximity of a nanostructured Au film [30] and, as shown more recently, when Au NPs are deposited on top of a layer of quantum dots [31]. As a continuation of this latter study, the energy transfer between a layer of QDs and nanostructured Au layers on spherical substrates

(latex microspheres) is presently being investigated. The spherical, nanostructured Au layers necessary for this investigation were prepared as part of this project. This was achieved by LBL adsorption of as-prepared Au NPs (above) onto MF lattices of different diameters (approx. 3, 5 and 10 μm) pre-coated with several polyelectrolyte layers.

Transmission electron microscopy of fabricated samples showed that a very smooth and dense coating of gold NPs on latex microspheres was achieved (fig. 5.3). Most likely, this can be attributed to the high concentration of colloidal gold solution used during the assembly process. All resultant samples were characterized by determining the average diameters of microspheres from the corresponding TEM images (table 5.1).

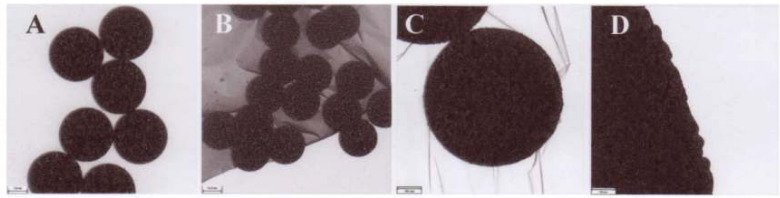

Fig. 5.3. TEM images of (a) 3μm, (b) 10μm and (c) 5μm MF lattices coated with gold NPs. (d) An edge of a 5μm Au-MF sphere.

SAMPLE	AVERAGE DIAMETER (μm)
3 μm	2.7 ± 0.2
5 μm	4.9 ± 0.3
10 μm	9.0 ± 1.4

Table 5.1. Average sizes of Au-MF structures. Sample names denote the approximate diameter of uncoated MF lattices.

5.2 Synthesis of Glycine-Stabilised CdSe

The microwave-assisted synthesis of CdSe nanocrystals have been previously reported [23] for the fabrication of citrate-stabilized CdSe QDs. The advantages of this method include its flexibility and ease of execution. However, citrate-stabilized NCs synthesized in this manner were found to have rather low quantum yields (<1%). In order to increase the QY of the nanocrystals prepared by this method, some parameters needed to be changed. We decide to attempt the fabrication of CdSe nanoparticles by substituting citrate by a different stabilizer – glycine. Glycine was chosen as it has –SH groups in its composition, which are frequently found in substances used to stabilize luminescent nanoparticles. Glycine is an amino acid, and as such, it might result in a reduced toxicity of CdSe QDs.

A number of glycine-stabilized CdSe nanocrystal solutions were synthesized, while varying either the Cd:Se ratio or the pH of solution, and monitoring the effects spectrally during the synthesis.

To vary the Cd:Se ratio, synthesis was performed using 4, 8 and 16mL of cadmium solution at pH 9, while keeping the amount of Se source constant. These volumes correspond to 4:1, 8:1 and 16:1 Cd:Se ratios respectively.

CdSe nanocrystals are well known for their size dependent luminescence. It was found that varying the ratio had a direct effect on the photoluminescence of the sample - the 8:1 Cd:Se sample had the highest luminescence, while no PL peak was observed for the 4:1 Cd:Se sample. Figs 5.4a and 5.4b show the normalized photoluminescence spectra[#] for the 8:1 and 16:1 Cd:Se samples respectively. Apart from the general increase of PL peaks with heating time, a red-shift in their positions was observed. This is characteristic of an increase of the average size of CdSe nanocrystals as they grow.

It should be pointed out that even for the 8:1 Cd:Se sample, the photoluminescence intensity was so small that the QY of CdSe NCs could not have exceeded 1%.

[#] All PL spectra were normalized based on the absorbance of the sample at excitation wavelength using PL(normalized) = PL(measured)/(1-10$^{-(\text{absorbance at excitation wavelength})}$).

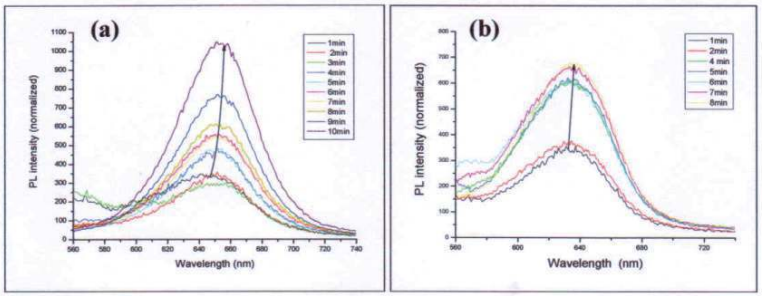

Fig. 5.4. The photoluminescence (PL) spectra for the synthesis of glycine stabilised CdSe NCs with (a) 8:1 and (b) 16:1 Cd:Se ratio used. The PL spectra was normalised based on the absorbance of the sample at 400nm using PL(norm) = PL(measured)*(1-10$^{-ABS\ at\ 400nm}$).

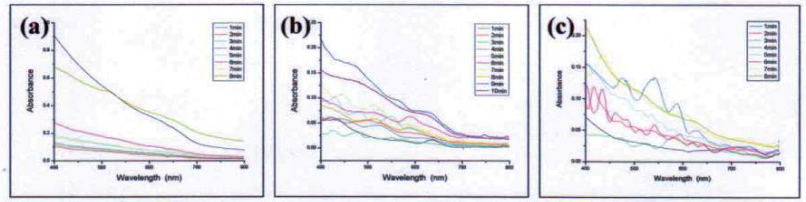

Fig. 5.5. The absorbance spectra of (a) 4:1, (b) 8:1 and (c) 16:1 Cd:Se samples. The "wave-like" features were attributed to the settling of the precipitate during scanning. Due to the evaporation of the solvent during synthesis, samples became progressively more concentrated with time. It was thus necessary to dilute the samples by different amounts when taking their absorbance spectra.

In all samples, and unlike the case of citrate-stabilised CdSe [32,33], a brown flake-like precipitate formed upon heating, while the solution itself remained more or less clear. The precipitate remained suspended for long periods of time, settling slowly after shaking. This settling, in addition to scattering by the precipitates, was responsible for the "wave-like" features observed in the absorption spectra of samples (shown in fig. 5.5). For 8:1 or 16:1 Cd:Se ratios used during the synthesis, the precipitates formed were clearer in colour and slightly suspended even without shaking.

The precipitates of all samples were examined using a transmission electron microscope (TEM). In general, large conglomerates were observed (fig. 5.6(a)). In fact, the sizes of these conglomerates were of the order of tens of microns, so that they can be easily observed with a naked eye as a flake-like precipitate. At higher magnification, however, these large conglomerates were found to be composed of nanorings and nanowires decorated by nanocrystals (fig. 5.6), the appearance and/or size of which differed depending on the conditions in which the synthesis was performed. This hints towards the possibility of controlling the morphology of CdSe samples by a simple adjustment of starting reaction parameters.

The nanowires/nanorings and the nanocrystals in 8:1 and 16:1 Cd:Se samples were, in general, smoother than those in the 4:1 Cd:Se sample, with the nanowires/nanorings having a more fibre-like appearance in these samples. The nanorings and the nanocrystals in 4:1 Cd:Se sample had a "hedgehog"-like appearance which was previously observed for citrate-stabilised CdSe NCs formed under same initial reaction conditions (i.e. same pH and Cd:Se ratio). Interestingly, the formation of nanorings was also found to be specific to these same reaction conditions as they were not observed for any other Cd:Se ratios or pHs of the reacting solutions.

The relative abundance of the nanocrystals also differed, with the 8:1 Cd:Se sample having the highest and the 16:1 Cd:Se sample having the lowest abundance. Almost all of the nanocrystals were confined to fibres in these two samples.

The nanoparticle sizes determined from these images are concurrent with the PL data. The particles in 4:1 Cd:Se sample had an average diameter of about 37nm and as such they were too large to show any photoluminescence. The average particle sizes in the other two samples, 8:1 and 16:1 Cd:Se, were about 6 and 4 nanometres respectively. CdSe particles of these sizes do luminesce.

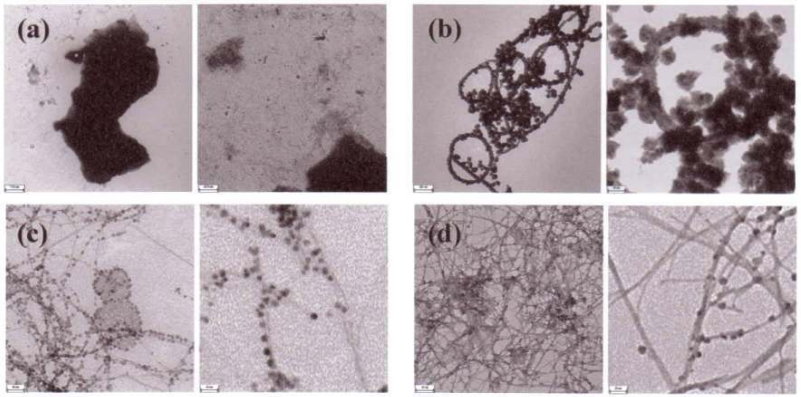

Fig. 5.6. TEM images of the (a) large conglomerates found in the precipitates, and higher magnification TEM images of these conglomerates for (b) 4:1, (c) 8:1 and (d) 16:1 Cd:Se samples.

The effect of varying the pH of the reacting mixture was studied by repeating the synthesis at pHs 7, 9 and 10. pH of 10 was the highest we were able to obtain – solution becomes unstable at this pH due to the hydrolysis of cadmium by NaOH. As a result of this any further addition of NaOH does not increase the pH of the solution. The samples obtained at pH 7 showed no photoluminescence, while those obtained at pH 9 (fig. 5.4a) had PL peaks of much higher magnitude than did those obtained at pH 10 (fig.5.7). This again is consistent with the data obtained from the TEM images of the precipitates. As before, large conglomerates were observed at low magnification. When these were examined in more detail, only aggregates of nanocrystals >100nm in size were observed for the pH7 samples (fig. 5.10(a)), thus explaining the lack of photoluminescence of these samples. Individual nanocrystals of about 5nm in diameter were observed for the pH10 samples (fig. 5.10(b)); however these also were mainly present as large aggregates. The relative abundance of individual nanoparticles in these samples was much less in that in those obtained at pH 9 (fig. 5.6(b)), which is in agreement with the relative magnitudes of the photoluminescence of these two samples.

When the CdSe synthesis was performed at pH10, white flakes formed first with the solution going clear brown, but leaving the sample overnight or continuing the heating both had the same effect of flakes acquiring a brown colour and the solution going colourless (fig. 5.8(b)).

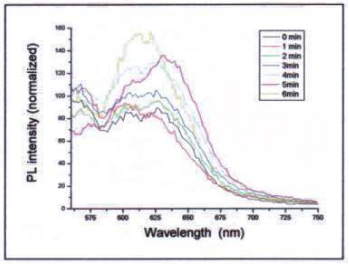

Above:

Fig. 5.7. PL of samples synthesized at pH 10.

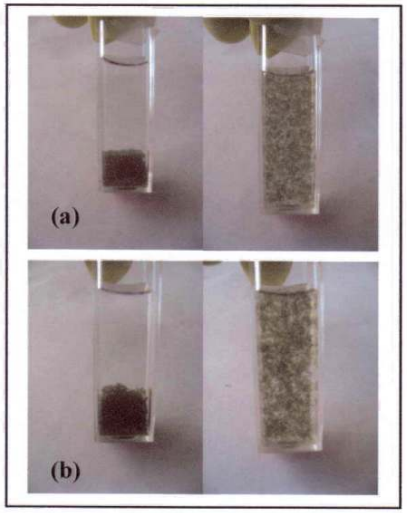

Right:

Fig. 5.8. Photographs of (a) pH7 and (b) pH10 samples.

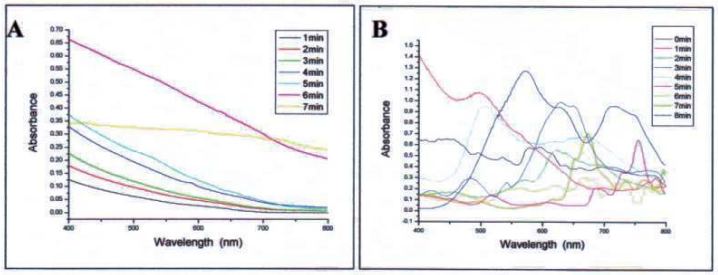

Fig. 5.9. The absorption spectra of (A) pH7 and (B) pH10 samples. The flakes in the pH10 samples settled very quickly, which explains the nearly random appearance of their absorption spectra.

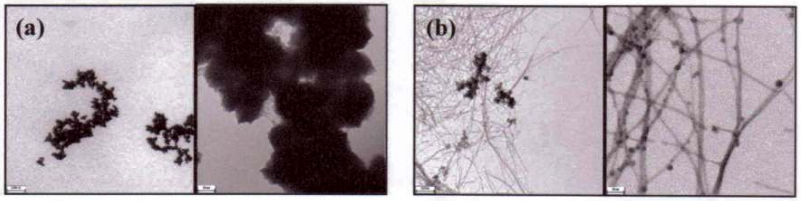

Fig. 5.10. TEM images of precipitates in (a) pH7 and (b) pH10 samples.

Two control experiments were also performed. This was done in an attempt to determine the nature of the flake-like precipitate that formed in all of the mentioned above synthesises. No photoluminescence was observed for any of the samples prepared under conditions used in either of these experiments as no CdSe nanocrystals formed.

The first experiment involved excluding either cadmium salt or selenium precursor from the reacting mixture. When no cadmium was added, the solution had a brownish colour but no precipitate formed. However, several days later a brown powder-like precipitate was noticed (fig. 5.11(a)) in all Se only samples. On the other hand, a flake-like precipitate was observed when Se precursor was excluded from the reaction mixture, however this precipitate was white (fig. 5.11(b)). Both of these precipitates were examined using TEM. Figure 5.12 shows some of the TEM images obtained. The fibre-like features seen previously in the other samples were observed for the samples prepared with no Se precursor added, but not for the samples where no Cd salt was present. This suggests that similar features in other samples were due to the hydrolysis of Cd, while the brown colour is due to some substance formed during the synthesis (which may or may not have Se in its composition).

Measurements of electrical and photoelectrical conductivity of some of the precipitates were next conducted. A. Biebersdorf et al. have previously showed that a weak photocurrent can be generated by CdSe nanocrystals. However, although the CdSe samples prepared by us were found to be very conductive, no photovoltaic response was detected.

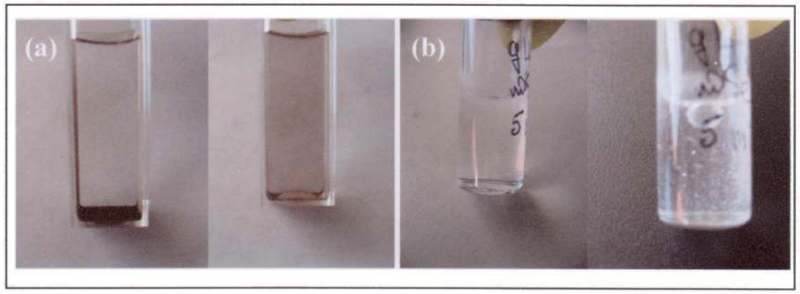

Fig. 5.11. Photographs of samples synthesised with (a) no Cd salt and (b) no Se precursor added.

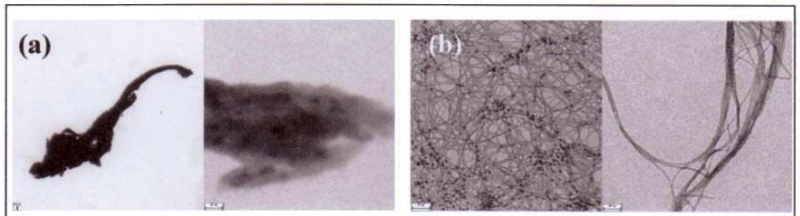

Fig. 5.12. TEM images of precipitates in (a) no Cd and (b) no Se samples.

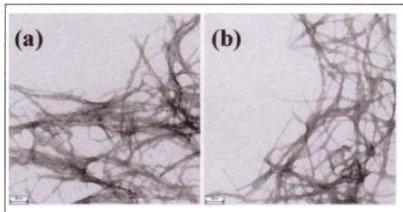

Fig. 5.13. TEM images of precipitates formed upon the hydrolysis of Cd in (a) water at pH7 and (b) glycine at pH10.

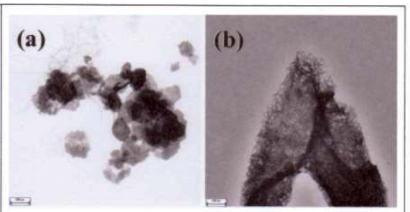

Fig. 5.14. Lower resolution TEM images of samples obtained from hydrolysis of cadmium in (a) glycine and (b) water.

In the second control experiment, the pH of the Cd salt solution in 1) glycine and 2) water was raised until the hydrolysis of cadmium started. This happened at pH 7 for Cd in water and at pH 10 for Cd in glycine. In both cases a white precipitate formed; the one formed as a result of the hydrolysis of Cd in water was powder-like, while the one formed in glycine had a flake-like appearance. Interestingly, when TEM images of these precipitates were taken at high magnifications, both samples had fibre-like features (see fig. 5.13) which were very similar to each other. This confirms that such features previously seen in other samples were due to the hydrolysis of cadmium, which would result in the formation of $Cd(OH)_x$. At lower magnifications these two samples differed in that for the hydrolysis of Cd in water only large conglomerates composed of fibres were observed, while for the hydrolysis of Cd in glycine resulted in a formation of nanoflakes as well as fibres (see fig. 5.14. for lower resolution TEM images). The formation of such nanoflakes was previously reported for the synthesis of cadmium hydroxide in aqueous media by hydrothermal method [34].

5.3 CdTe Nanocrystals

5.3.1 Synthesis of CdTe NCs

Properties of CdTe nanocrystals are very sensitive to the nature of the stabiliser [22]. As a result, particle growth, and also their charge, photoluminescence efficiency and biocompatibility, can be easily controlled by choosing appropriate stabiliser. The discovery of new stabilisers is important as it broadens the range of nanocrystal properties, and hence also the range of their applications. Thus, α-lipoic acid (LA) and sodium 2-mercaptoethanesulphonate (MES), whose structures are shown on the right, were tested as stabilisers using an already well-established method of CdTe NC preparation [22].

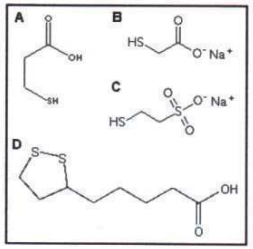

Fig. 5.15 Chemical structures of well known stabilizers (A) MPA and (B) TGA, and investigated (C) MES and (D) LA.

For both substances, two test syntheses were first performed. The reaction conditions for these syntheses were: 1) Cd:Stabiliser ratio of 1:2.15 and a pH of 11.2, and 2) Cd:Stabiliser ratio of 1:1.5 and a pH of 12. Such reaction conditions were chosen as they are the most extensively used reaction conditions for the synthesis of highly luminescent TGA-stabilised CdTe NCs. The growth (or otherwise) of particles was monitored by recording both the absorption and the photoluminescence spectra of solutions taken out from the refluxing mixture at different intervals of time.

Lipoic acid was chosen as it might have led to the possibility of biocompatible-QD production with a stronger attraction towards the CdTe surface by two sulphur atoms (relative to TGA). In addition, it has the same free organic group (FOG) as do common stabilisers MPA and TGA.

However, a number of difficulties were encountered when test syntheses of MA-stabilised CdTe NCs were attempted. First of all, LA was found to be only partially solvable in water at room temperature. This presents a problem at the initial stages of the synthesis (e.g. the dearation of the system). Lipoic acid dissolved completely upon heating, and the reacting mixture was slightly coloured but clear at the start of the reflux stage of synthesis. However, as heating continued, a precipitate formed. Neither this precipitate nor the solution was found to be luminescent.

Next, test syntheses of MES-stabilised CdTe NCs were attempted. MES was promising as it has an –SH group frequently found in luminescent particles' stabilisers. Furthermore, its SO_3^- FOG perhaps could have resulted in a more negative surface charge of CdTe nanocrystals as compared to TGA-stabilised colloidal CdTe. Both of test syntheses were successful and lead to the formation of luminescent CdTe nanoparticles. According to Peng [35], 3.7nm and 4.0nm dots CdTe NCs were produced as a result of test syntheses 1 and 2 respectively. This calculation uses the size dependence of the wavelength of the first excitonic absorption peak of CdTe nanocrystals.

Fig. 5.16A shows absorption and photoluminescence spectra measured on as-prepared CdTe solutions synthesised at pH 11.2 and a Cd:Stabiliser ratio of 1:2.15. The growth of the particles (with continued heating) was apparent through a shift of both the absorption maximum of the first electronic transition and the maximum of the photoluminescence peak (Figs. 5.16 A and B). A fast growth was observed initially, with photoluminescence peak shifting from 540nm to 570nm in a matter of 2 hours. However, the rate of the growth slowed down considerably after this initial stage, and during the last 20 hours of the synthesis a peak shift of only 9nm was detected. An even faster initial growth rate was observed under higher pH and lower Cd:Stabiliser ratio (i.e. test synthesis 2). At these conditions, PL peak shifted by 60nm during the first 3 hours of the refluxing, and only by 4nm during the last 20 hours (Fig. 5.16 B, red circles). In general, such growth profile is typical for aqueous colloidal CdTe fabrication.

The next aim of the project was to synthesize samples of CdTe NCs emitting in the red and green using "standard" conditions described above. The growth of QDs emitting in the green under test synthesis 2 conditions would have been challenging because of the fast initial growth of CdTe nanocrystals (see fig. 5.16 B). Under these conditions, the growth of the NC must be stopped (at most) ~15 minutes after the start of the reflux. However, considering that growth proceeds for a while after the reaction mixture stopped boiling, and that very poor quality NCs would have resulted from such a synthesis, the fabrication of green QDs is not practical (if not impossible) under these conditions. On the other hand, the very fast initial growth is advantageous for the production of red QDs. In consequence, the reaction conditions of test syntheses 1 and 2 were used to produce crude solutions of green and red CdTe QDs respectively, both of which were subjected to size-selective precipitation treatment. For this treatment, a procedure identical to that used for the fractionation of TGA-stabilised CdTe NCs was tested, and found to be successful.

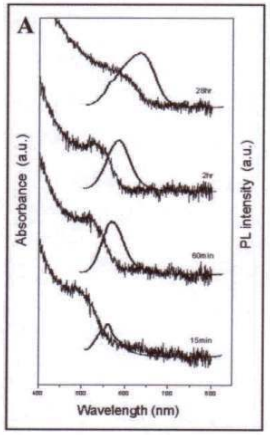

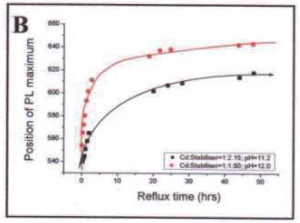

Fig. 5.16 Test syntheses of MES-stabilised CdTe QDs:

A. Absorption and photoluminescence spectra of some CdTe samples as prepared at pH=11.2 and a 1:2.15 Cd:Stabiliser ratio.

B. The change in the position of the photoluminescence peak maximum with refluxing time. Black squares: 1:2.15 Cd:Stabiliser ratio and a pH of 11.2synthesis. Red dots: 1:1.50 Cd:Stabiliser ratio and a pH of 12.0 synthesis.

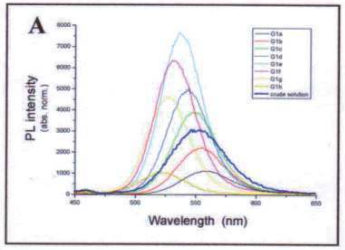

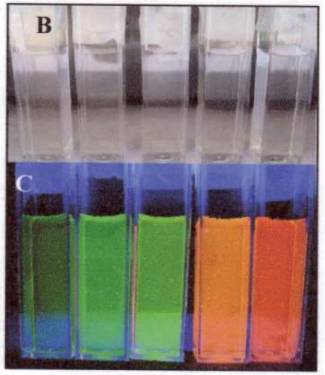

Fig. 5. 17. (a) Photoluminescence spectra and photographs of fractions obtained from crude solution of green QDs (b) under sunlight and (c) under UV light.

Sample	Calculated size (nm)	Hydrodynamic size - measured (nm)	Average zeta potential (mV)	Conductivity (mS/cm)
Green fraction *g*	<3.0	3.13	-51.6	0.54
Red fraction *e*	3.9	5.54	-57.0	0.16

Table 5.2. Zeta potential and size data measured using a Malvern ZEN3600 ZetaSizer. Calculated diameters of NCs are given for comparison. Conductivity values are shown because zeta potential of a sample depends on its conductivity.

Fig. 5.17 A compares the photoluminescence spectra of the crude green QD solution and that of its fractions. The photoluminescence peak of first fractions is red-shifted compared to that of the crude solution, while the PL peaks of the last fractions are blue-shifted. This is because the heavier, and hence larger, nanocrystals precipitate first during the fractionation. The narrowing down of NC size distribution upon fractionation is also notable from fig. 5.17 A through the narrowing down of the corresponding photoluminescence peaks. From the crude red QD solution, several fractions of NCs emitting at ~700nm were obtained. This is important to specify since TGA-stabilised CdTe NCs cannot be grown to emit in this region without the injection of additional precursors.

The mean size of NCs in any particular fraction can be calculated according to Peng [35]. Here, the values of <3.0nm obtained for fraction *g* of the green QD series, and 3.9nm for fraction *e* of the red QD series are reported since zeta potential and hydrodynamic size measurements were performed on these samples. The size data obtained from these measurements are summarised in table 5.2. In general, the measured values were greater than predicted, but this is to be expected since hydrodynamic size is always larger than the hardcore diameter of NCs. It should also be noted that the values given in this table are the smallest average values obtained. In general, larger populations were also observed – these were aggregates of NCs.

As already mentioned above, we expected that the more electron withdrawing SO_3^- group of MES (as compared to CO_2^- of TGA) would have lead to a more negative surface charge of MES-stabilized CdTe NCs. To test whether this was in fact the case, zeta potential measurements were performed on two fractions mentioned above.

Zeta potential relates to the stability of NCs as colloids and depends on a number of factors which include the charge of colloidal particles and the conductivity of the solvent. Thus, higher surface charge results in higher zeta potential. Both of the investigated samples had negative zeta potentials (table 5.2) with values comparable to that of TGA-stabilised CdTe (typical value of a TGA sample with a conductivity of 0.20 mS/cm is about -50mV). From this a conclusion can be made that MES-stabilised CdTe NCs have a negative surface charge. It should be mentioned that zeta potential values given in table 5.2 are averages, in fact values as low as -77mV were measured. This is in accordance with the expectation outlined above suggesting that the surface charge of MES–stabilized QDs may in fact be more negative than that of TGA-stabilized CdTe.

Next, several other syntheses were carried out under different reaction conditions in order to investigate their effects: pH, Cd:Stabiliser ratio and Cd:Te ratios were changed. The three sets of reaction conditions used, and also samples obtained under each set of reaction conditions, are given in table below (table 5.3). For all of these syntheses precipitates formed. For syntheses 1 and 2, this happened in the first 30 minutes of the reflux. For synthesis 3, it occurred at some time between 4 and 19 hours of refluxing (this occurred overnight and hence the exact point is not known). Surprisingly, these precipitates, as well as the solutions, were found to be highly luminescent (fig. 5.18).

The quantum efficiencies of all solutions were measured by comparison with Rhodamine 6G standard (QY of 95%). Values as high as 39.6% were obtained (see table 5.4). Judging by the photoluminescence spectra of solution/precipitate pairs (e.g. fig. 5.19), the quantum efficiencies of precipitates were, in general, approximately half those of the corresponding solutions. However, such approach underestimates the QY of precipitates since they are very strong scatterers of light (even at high dilutions).

Fractionation of three synthesized solutions was attempted. The evaporation of solvent from the first solution - the result of a 4.5hour reflux under synthesis 2 conditions - lead to the precipitation of all NCs. These were still luminescent in the precipitate (QY=11.3%). Successful fractionation was realized with both of the samples fabricated under synthesis 3 conditions (fig. 5.20). QYs of fractions of synthesis 3, 1hr sample were measured. The highest value of 23% was obtained for the 3rd fraction (*c*), as compared to ~9% of the crude solution.

Transmission electron microscopy was performed on several of the more luminescent precipitates; however, most images obtained were inconclusive due to poor contrast. Also, very few QDs were observed.

Name	Reaction conditions	Samples refluxed for
Synthesis 1	pH = 11.2; Cd:MES = 1:1.5; Cd:Te = 3.43:1	1.5, 2.5 and 4 hours
Synthesis 2	pH = 11.2; Cd:MES = 1:1.5; Cd:Te = 1.85:1	1 and 4.5 hours
Synthesis 3	pH = 12.0; Cd:MES = 2.15; Cd:Te = 1.53:1	1 and 22 hours

Table 5.3. Investigatory syntheses, their reaction conditions and samples obtained.

Synthesis 1		Synthesis 2		Synthesis 3	
1.5 HR sample:	*39.6%*	1 HR:	*16.8%*	1 HR:	*8.9%*
2.5 HR:	*27.6%*	4.5 HR:	*12.6%*	22HR:	*4.7%*
4 HR:	*18.3%*				

Table 5.4. Quantum yields of solutions of different samples (± 0.1%).

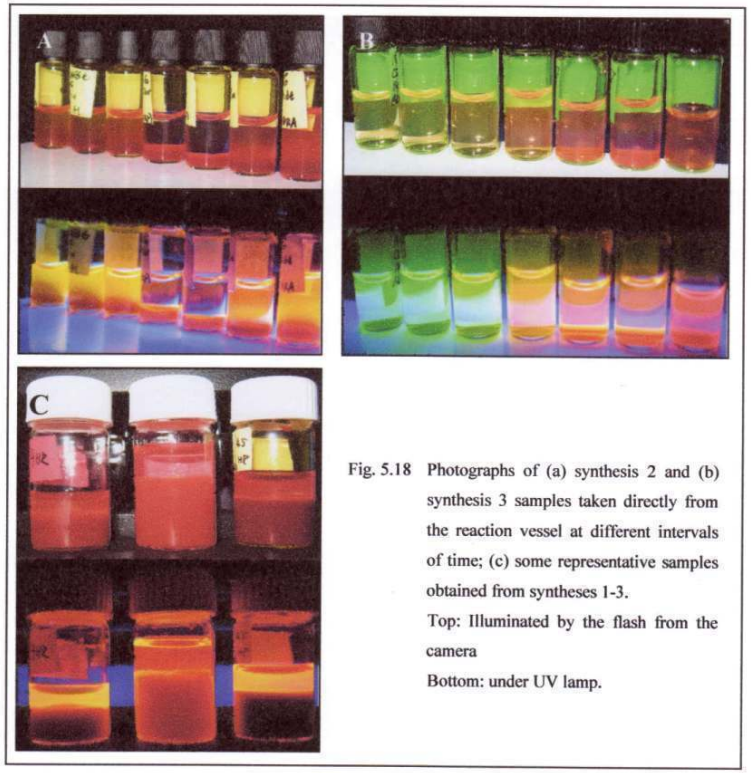

Fig. 5.18 Photographs of (a) synthesis 2 and (b) synthesis 3 samples taken directly from the reaction vessel at different intervals of time; (c) some representative samples obtained from syntheses 1-3.
Top: Illuminated by the flash from the camera
Bottom: under UV lamp.

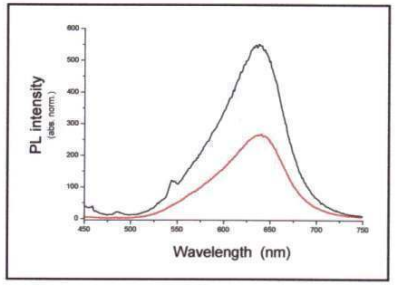

Fig.5.19. Representative PL spectra of solution(-)/precipitate(-) pair.

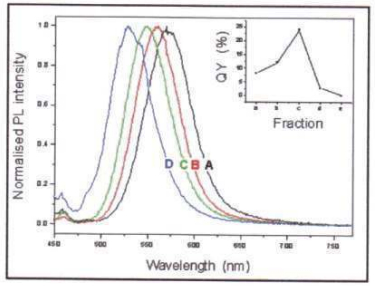

Fig. 5.20. Normalised PL spectra of a-d fractions of synthesis 3, 1hr sample. The inset shows the quantum efficiencies of these fractions.

5.3.2 LBL Assembly of CdTe NCs on Latex Microspheres

Energy transfer was previously shown to be possible in structures comprised of monolayers of differently sized CdTe QDs [36]. A very fast and efficient cascaded energy transfer was reported for a structure in which a funnel-like band gap variation was achieved by stepwise alternation of QDs sizes in subsequent layers [37]. Hitherto, such energy transfer was only described for layers of NCs on planar substrates. The aim of this part of the project was thus to realise such structures on a spherical substrate, in particular, on latex microspheres. Luminescent latex microspheres are already commonly used as bio-labels. Cascaded energy transfer in proposed structures, if achieved, would greatly improve the intensity of these bio-labels.

A preliminary study was first conducted which involved the fabrication and characterisation of structures consisting of 4 layers of QDs. This was accomplished by a LBL assembly of red (R, λ_{max}=613 nm) and green (G, λ_{max}=555 nm) TGA-stabilized CdTe NCs on PS lattices. Two reference samples consisted of 4 layers of only green and only red QDs, while in the test sample the green and red layers were alternated.

All three samples were characterised by recording their PL spectra[#]. No photoluminescence was detected for any of the samples. Here, it should be mentioned that since both the adsorption of NC and PE layers and also the subsequent washing are rather time-consuming processes, the fabrication of such 4-layered samples takes 2 days. All samples were checked for luminescence at the end of first day of the synthesis (this corresponds to 2 deposited layers) by simply placing them in front of a UV lamp. All three samples were found to be luminescent. It was therefore peculiar that no PL was detected at the end of the fabrication process.

Visually, a change in colour was observed from white (starting solution), to orange or red after the deposition of first green or red layers respectively, and to grey (final samples). This, together with the loss of photoluminescence, is indicative of the degradation of samples within 24 hours since the start of fabrication.

[#] The scattering from latex spheres is so strong that it dominates by far the absorption of the sample. Thus, the absorbance spectra of any of the described here samples were not recorded.

To test this conclusion, 2-layered structures were next produced (diagram 5.1), and their PL spectra were recorded immediately after their fabrication. No PL peak for green QD sample was observed, which may be due to the combination of a small amount of dots adsorbed and their relatively low QY. A weak photoluminescence was detected for red only and also composite samples (fig.5.21).

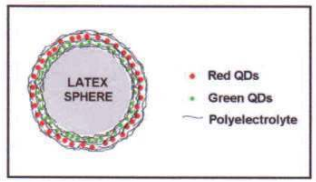

Diagram 5.1 A schematic representation of the 2-layered composite sample.

However, the normalisation the photoluminescence based on the absorbance of the samples at the excitation wavelength was not possible due to the strong scattering by latex microspheres. As a consequence of this, as well as the low QY of green dots, we were unable to conclude whether any cascaded energy transfer has occurred.

The photoluminescence of these three samples was measured again 12 hours later. No photoluminescence was detected for any of the samples, which confirmed the above hypothesis of sample degradation. This degradation could be due to some interaction of surface atoms of NCs with polyelectrolytes. This would be concurrent with the luck of PL of 2-layered green only sample since green QDs have higher ratio of surface to bulk atoms. They would therefore interact more strongly with the PEs, and so their photoluminescence would decay faster.

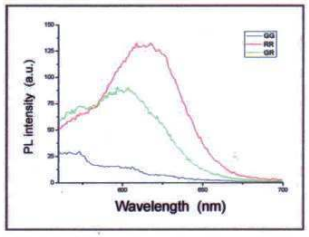

Fig. 5.21. Photoluminescence spectra of 2-layered structures recorded immediately after the fabrication.

6. Summary and Conclusions

This project consisted of three parts involving synthesis, and in some cases assembly, of gold nanoparticles, CdSe NCs and CdTe NCs.

Highly concentrated aqueous colloidal gold was produced by a two-step synthesis. Gold NPs had an average diameter of ~4.7nm with a standard deviation of 1.3nm, as was determined from the transmission electron microscopy. Fabricated nanoparticles were subsequently adsorbed onto MF latex microspheres of different diameters by a LBL technique. Such gold-MF microspheres were produced for further studies of enhancement/quenching of semiconductor nanocrystal photoluminescence.

In the second part of the project, the microwave-assisted synthesis of glycine-stabilised CdSe NCs was investigated. Different reaction conditions (Cd:Se ratios or the pH of the reacting mixture) were tested. In all cases precipitates formed, which were identified to be large conglomerates of nanorings/nanowires decorated by CdSe nanocrystals. The formation of these nanorings and nanowires was attributed to the hydrolysis of cadmium. It was found that the morphology of the samples could be controlled on the nanoscale through the adjustment of initial reaction conditions. However, the QY of any of the produced samples did not exceed 1%. This is a drawback of the microwave-assisted synthesis.

Next, lipoic acid and sodium 2-mercaptoethanesulphonate (MES) were investigated as potential stabilisers for aqueous CdTe NCs. Based on two test syntheses, lipoic acid is not suitable for use as CdTe NCs stabilisers; however, syntheses of MES-stabilised CdTe NCs were successful. Various syntheses of such QDs were performed under various reaction conditions, their growth was monitored spectrally. Some of the fabricated samples were fractionalised by a method identical to the one used for the fractionation of TGA-stabilised QDs. According to zeta potential measurements, MES-stabilised CdTe NCs have negative surface charge comparable to, or possibly, even more negative than that of the TGA-stabilised QDs. The highest QE of crude, as-prepared, MES CdTe solution was 39.6%. This again is similar to typical highest values reported for TGA CdTe. Highly luminescent precipitates, with underestimated QYs of up to 15%, formed under certain reaction conditions. Potentially, this could be useful for some applications.

Finally, an attempt was made to produce structures consisting of monolayers of differently sized NCs on latex microspheres by a LBL assembly method. However, samples were found to degrade as manifested through the quenching of their photoluminescence.

7. References

[1] *Structure and Photophysics of Semiconductor Nanocrystals*, A. Eychmüller, J. Phys. Chem. B 2000, 104, 6514-6528

[2] *New aspects of Nanocrystal Research*, L.M. Liz-Marzán, D.J. Norris, December 2001, MRS bulletin, 981-982

[3] *Optical Properties of Metal Clusters*, Uwe Kreibig, M. Vollmer, 2nd edition, 1995, Springer-Verlag.

[4] *Optical Properties of Semiconductor Nanocrystals*, S.V. Gaponenko, Cambridge University Press, Cambridge 1998.

[5] *Colloids and colloid assemblies : synthesis, modification, organization and utilization of colloid particles*, Chapter 2, edited by Frank Caruso, Wiley-VCH, 2004

[6] *Colloids and colloid assemblies : synthesis, modification, organization and utilization of colloid particles*, Chapter 3, edited by Frank Caruso, Wiley-VCH, 2004

[7] M. Faraday, Philos. Trans. R. Soc. London, 1857, 147, 145

[8] *A study of the nucleation and growth processes in the synthesis of colloidal gold*, J. Turkevich, P.C. Stevenson, J.H. Hillier, Discuss. Faraday Soc., 1951, 11, 55

[9] *Experiments in Colloidal Chemistry*, E.A. Hauser, J.E. Lynn, McGraw Hill, New York, 1940

[10] R. Zsigmondy, Z. Phys. Chemie, 1906, 56, 65

[11] *Why gold nanoparticles are more precious than pretty gold: Noble metal surface plasmon resonance and its enhancement of the radiative and nonradiative properties of nanocrystals of different shape*, S. Eustis, M. A. El-Sayed, Chem. Soc. Rev. 2006, 35, 209-217

[12] *Adsorption of Bifunctional Organic Disulfides on gold surfaces*, R.G. Nuzzo, D. L. Allara, J. Am. Chem. Soc., 1983, 105, 4481-4483

[13] *Preparation of Ordered Colloid Monolayers by Electrophoretic Deposition*, M. Giersig, P. Mulvaney, Langmuir, 1993, 9, 3408-3413

[14] *Synthesis of Thiol-Derivatized Gold Nanoparticles in a 2-Phase Liquid-Liquid System*, M. Brust, M. Walker, D. Bethel, D.J. Schiffrin, C.J. Kiely, J. Chem. Soc., Chem. Comm., 1994, 801-802

[15] *Gold nanoparticles: Assembly, supramolecular chemistry, quantum-size-related properties, and applications toward biology, catalysis, and nanotechnology*, M.C. Daniel, D. Astruc, Chem. Rev., 2004, 104, 293-346

[16] *Utilization of Surfactant-Stabilized Colloidal Silver Nanocrystallites in the construction of Monoparticulate and Multiparticulate Langmuir-Blodgett-Films*, F.C. Meldrum, N.A. Kotov, J.H. Fendler, Langmuir, 1994, 10, 2035-2040

[17] *Large Transition-Metal Clusters .6. Ligand-Ecxhange Reactions on Au55(PPh3)12Cl6 – the Formation of a Water-Soluble Au55 Cluster*, G. Schmid, N. Klein, L. Korste, U. Kreibig, D. Schönauer, Polyhedron, 1988, 7, 605-608

[18] *Semiconductor Nanocrystals as Fluorescent Biological Labels*, M. Bruchez, M. Moronne, P. Gin, S. Wiess, A.P. Alivisatos, Science, 1998, 281, 2013-2016

[19] *Spontaneous Phase Transfer of Nanoparticulate Metals from Organic to Aqueous Media*, D.I. Gittins, F. Caruso, Angew. Chem. Int. ed. 2001, 40, 3001-3004

[20] *Photochemistry of Colloidal Cadmium-Sulfide .2. Effects of Adsorbed Methyl Viologen and of Colloidal Platinum*, A. Henglein, J. Phys. Chem., 1982, 86, 2291-2293

[21] *Synthesis and Characterization of Nearly Monodisperse CdE (E = S, Se, Te) Semiconductor Nanocrystallites*, C.B. Murray, D.J. Norris, M.G. Bawendi, J. Am. Chem. Soc. 1993, 115, 8706-8715

[22] *Thiol-Capping of CdTe Nanocrystals: An Alternative to Organometallic Synthetic Routes*, N. Gaponik et al., J. Phys. Chem. B 2002, 106, 7177-7185

[23] *„Raisin Bun"- Type Composite Spheres of Silica and Semiconductor Nanocrystals*, A. L. Rogach et AL, Chem. Mater. 2000, 12, 2676-2685

[24] G. Decher, J.-D. Hong, Makromol. Chem. Macromol. Symp. 1991, 46, 321

[25] *Fuzzy Nanoassemblies: Towards Layered Polymeric Multicomposites*, G. Decher, Science 1997, 277, 1232

[26] *Fluorescence Quantum Yields of Some Rhodamine Dyes,* R.F. Kubin, A.N. Fletcher, J. Luminesc. 1982, 27, 455-462

[27] *Semiconductor Nanocrystals Photosensitize C_{60} Crystals*, A. Biebersdorf et al., Nano Lett. Vol. 6, No. 7, 2006, p. 1559-1563

[28] *Magnetic Core-Shell Paticles: Preparation of Magnetite Multilayers on Polymer Latex Microspheres*, F. Caruso et AL, Adv. Mater. 1999, 11, 950-953

[29] *Dense Nanoparticulate Thin Films via Gold Nanoparticle Assembly*, D.I. Gittins et AL, Adv. Mater. 2002, 14, 508-512

[30] *Off-resonance surface plasmon enhanced spontaneous emission from CdTe quantum dots*, V.K. Komarala, Y.P. Rakovich, A.L. Bradley, Yu.K. Gunko, N. Gaponik, A. Eychmüller, Appl. Phys. Lett. 2006, 89, 253118

[31] *Imaging of Quenched Luminescence of Quantum Dots by Nanostructured Gold Nanoparticles*, A.M. Raighne, Y. Rakovich, E. Mc Cabe, proc. of Quantum Electronics and Photonics (QEP-17) 2006, p2.6

[32] *Decorated Nanowires, Nanorings and "Hedgehog-Like" Superstructures Containing CdSe Nanocrystals, Produced by Microwave-Assisted Synthesis* – Poster presentation at CeNS workshop (September 2006, VIU, Venice, Italy) titled "Emerging Nanosystems – From Quantum Manipulation to Nanomachines", A.S. Susha at AL.

[33] Paper pending

[34] *Synthesis of Cadmium Hydroxide Nanoflake and Nanowhisker by Hydrothermal Method*, H. Zhang et al., Mat. Lett. 2005, 59, 56-68

[35] *Experimental Determination of the Extinction Coefficient of CdTe, CdSe, and CdS Nanocrystals*, X. Peng et AL., Chem. Mater. 2003, 15, 2854-2860

[36] *Spectrally Resolved Dynamics of Energy Transfer in Quantum-dot Assemblies: Towards Engineered Energy Flows in Artificial Materials*, V.I. Klimov et Al., Phys. Rev. Lett. 2002, 89, 186802

[37] *Exciton Recycling in Graded Gap Nanocrystal Structures*, T.A. Klar et al., Nano Lett. 2004, 4, 1559-1603